CLM-R242

CLM-R242

UKAEA

Report

THE PEAK TOROIDAL FLUX DENSITY REQUIRED AT VARIOUS STAGES IN THE PROGRAMME OF TOKAMAK DEVELOPMENT

W. R. SPEARS

CULHAM LABORATORY
Abingdon Oxfordshire

1983

C/18 Available from H. M. Stationery Office £5.00

CLM-R242

THE PEAK TOROIDAL FLUX DENSITY REQUIRED AT VARIOUS STAGES IN THE PROGRAMME OF TOKAMAK DEVELOPMENT

W.R. Spears

Culham Laboratory, Abingdon, Oxon OX14 3DB, UK
(Euratom/UKAEA Fusion Association)

ABSTRACT

The incentives, risks and benefits associated with the development of high toroidal field coil systems to satisfy the aims of various devices in the tokamak development programme are investigated. An assessment is made by examining the parameter space available to devices with specific programme aims by using a simple model relating physical and technological parameters with cost. The results are sensitive to both physics and engineering assumptions, but insensitive to the scaling of magnet costs themselves with field. The most critical parameter determining the need for flux densities at or beyond 12 T is the blanket and shield thickness needed for adequate tritium breeding and efficient electricity generation.

September 1983

ISBN O 85311 1251

1. INTRODUCTION

It has long been an aim of the tokamak development programme to maximise the plasma power density in a reactor. This recognises qualitatively that high plasma power densities are necessary to reduce electricity costs in devices of a reasonable power rating [1]. Since plasma power density scales with the fourth power of the toroidal field, a vigorous development programme has been undertaken worldwide aimed at maximising the technically attainable field. It is important, however, to be aware of how strong an incentive there is for attaining high fields, so that time and effort will not be wasted in producing higher fields than will eventually be necessary to provide conditions conducive to economic power generation. This incentive is therefore quantified in this report.

Three steps in the tokamak development programme are likely: TNS (The Next Step), DEMO (Demonstration Power Producer) and the first CTR (Commercial Tokamak Reactor). The relevant objectives of these devices [2,3] are:

TNS: To take the largest reasonable step in plasma physics beyond the present generation of large tokamaks (e.g. JET) and demonstrate the plasma performance needed in DEMO;
To produce reactor-relevant particle and heat fluxes (mean neutron wall loadings above 1 MW/m^2) and accumulate 5 MWy/m^2 for component and materials testing;
To test, develop and integrate into a reactor system those technologies required for DEMO, i.e. blanket, tritium, plasma engineering, remote maintainability, reliability, safety and environmental acceptability.

DEMO: To produce net electrical power with net tritium breeding;
To demonstrate the development of compatible systems and components which can be extrapolated to a CTR;
To demonstrate component, materials and system lifetime at an acceptable level for a CTR;
To demonstrate safe, environmentally acceptable operation suitable for a CTR;
To demonstrate the economic feasibility of a commercial

reactor without the need for economic electricity production in DEMO itself.

CTR: To demonstrate power production at a competitive cost;
To operate reliably and safely with high availability;
To confirm the choice of materials and components;
To confirm the operation of remote maintenance logistics;
To convince electricity suppliers and consumers that tokamak fusion is ready for exploitation.

The parameters, particularly toroidal field, necessary to satisfy these objectives are described in the following sections.

Previous studies [4] have shown that higher fields may be needed to achieve adequate wall loadings in TNS devices than will eventually be required for commercial power reactors. This raises the question of what problems and risks are associated with not developing high field magnets and how do they compare with the benefits if such magnets are developed. The sensitivity of these risks and benefits to plasma physics assumptions must also be determined.

This report quantifies these risks and their sensitivities by assessing how high the peak toroidal field in a tokamak must be at each step in the tokamak development programme. Using INTOR [3] as an example of a TNS device, the implications of the high field specified in INTOR for the device objectives of DEMO and CTR are analysed. Conversely, the implications for TNS device objectives of fields only high enough for DEMO and CTR are also investigated. These assessments are carried out by examining the parameter space available to each device, based on a simple reactor model interrelating physical and technological parameters and cost per unit power (useful when commercial designs are compared) or total cost. This model is described in the following section.

2. MODEL DESCRIPTION

The main equations and assumptions of the simple model are shown in Table I. A glossary of symbols is given at the end of this report. Essentially, the model relates the capital cost per

TABLE I SIMPLE TOKAMAK REACTOR SCALING MODEL

(1) $P_T = \int_V \frac{n^2}{4} \langle\sigma v\rangle E_R dV$

(2) $\beta^* = \frac{4\mu_o}{B_o^2} \left[\int_V n^2 k^2 T^2 \, dV / \int dV\right]^{\frac{1}{2}}$

$$\Longrightarrow \quad P_T = F \left[\frac{\pi^2 E_R}{32\,\mu_o^2} \frac{\langle\sigma v\rangle}{k^2 T_n^2}\right] \beta^{*2} B_o^4 \, Ra^2 e \qquad (A)$$

F is a factor to account for density and temperature profile effects and F = 1 for flat profiles. Using

(3) $B_1 = \frac{B_o R}{(R-a-t/2)}$ (4) $\beta^* = \left(2.4 \frac{a}{R}\right)^{2-x} \frac{e}{1.6} \beta^*_{JET}$

(5) $P_w = \frac{P_T \sqrt{2}}{4\pi^2 Ra (1+e^2)^{\frac{1}{2}}}$ (6) $K = \frac{ct[t + a\,(1+e)]}{\sqrt{2}\, a\, P_w\, (1+e^2)^{\frac{1}{2}}}$

in equation (A), for B_o, β^*, R and a respectively leads to:

$$\frac{\alpha K^2 - \gamma K + \delta}{(\lambda K - \mu)^{17/4-x}} = \eta \qquad (B)$$

where $\alpha, \gamma, \delta, \mu, \lambda$ (P_T, P_w, e, c, t)
and η(P_T, P_w, e, c, t, x, F, β^*_{JET}, B_1)

In addition the following parameters are useful:

(7) $\tau_E = 5 \times 10^{-21} \bar{n} a^2 e$ (8) $I_p = \frac{B_o}{q_I} \frac{2\pi}{\mu_o} \frac{a^2}{R} \frac{(1+e^2)}{2}$

(9) $B_c = \frac{\mu_o R I_p}{2\pi\,(R-a-t)^2} \left[\ell n \left(\frac{8R}{a\sqrt{e}}\right) - 1.75\right]$

unit thermal power generated to the peak toroidal field at the coil, for a fixed set of physical and technological assumptions. The capital cost is derived on the basis of a fixed cost per unit of engineered volume (equation 6). This is taken here to be £250,000/m^3 - a value appropriate for the Culham MkIIB reactor [5,6]. The engineered volume is the volume of material surrounding the plasma, occupied by the blanket, shield and coil systems. For simplicity the engineered volume thickness is assumed to be constant on all sides of the plasma.

Clearly, costing on the above basis can only provide crude guidance to trends in cost improvement - for example, any costs not scaling with the engineered volume are ignored here and would need to be added in to arrive at the total capital cost. (Typically the engineered volume costs are about half the total capital cost [5]). Also, by implication, coil costs are treated as scaling with their volume only, rather than with field or with major radius, as is more likely [7,8], and this produces an underestimate of the cost of high field systems. The effect of this inaccuracy has been dealt with in more detailed studies [9] but, as is shown in section 4, the effect of incorporating a detailed coil cost scaling in this model does not change the strength of incentives sufficiently to justify the additional complexity of the model. Therefore, despite both these inaccuracies, the simple, volume-cost model is used here to show the strength of the incentive for using high fields in tokamaks. It should be recognised that the benefits of high field systems are likely to be exaggerated, but not sufficiently to change the conclusions.

To set the physics attained in a reactor in the perspective of what can be envisaged today, equation 4 is used to relate reactor β^* to the value obtained by "present day" experiments. The JET experiment is used here as an example. An implicit assumption is that poloidal beta scales with the 'x'th power of plasma aspect ratio. The value of x used in the study (1.0) is that appropriate for INTOR data under the assumption of a constant of proportionality of 0.6. This scaling was also used in the FED design study [10] and is borne out by more detailed studies of plasma equilibria [11] with optimised profiles. The value of the constant of proportionality has no bearing on the

model of Table I since the same constant must apply to JET. The results of this study are affected by the value of x, however, and this is examined further in section 5.

Equation A, on which the model depends, is corrected for density and temperature variation across the plasma in order to give the correct thermal power output defined in equation 1, and this is achieved by means of the function F. It is assumed that profiles of density and temperature are given by $n = n_o [1 - (r/a)^2]^{\nu_n}$ and $T = T_o [1 - (r/a)^2]^{\nu_T}$. Typical values of $F(\nu_n, \nu_T)$ at a T_n of 10 keV are given in appendix A and have been used throughout this study.

For a single valued right-hand side in equation B there are in general two meaningful solutions for cost. Thus, with all else fixed, two reactor designs are available for a given peak toroidal field. One design has low on-axis toroidal field, low aspect ratio and high β^*. The other uses high on-axis toroidal field, is high aspect ratio and hence of low β^*. Further distinctions may be made between such designs considering energy confinement time (ALCATOR scaling), plasma current and peak air-cored transformer core field (assuming a symmetric flux swing). These are included for discussion later.

3. INTOR - A TEST CASE

As an illustrative example, the model has been used to produce the INTOR [2] design point. Since INTOR is at an early stage of development several parameters necessary to fit the design to the model of table I are not available in the literature and must be deduced. The assumptions necessary to make use of INTOR as a suitable reference point for this study are therefore discussed in Appendix B.

Table II displays the resulting parameters of the INTOR reference point. The first section of the table contains basic, firm parameters of the INTOR design. The second section contains derived parameters. The high fraction of impurities and alpha particles (f_I) comes from standard definitions of β and n (Appendix B). To match the power output, $\bar{n}$ must refer to fuel ions only whereas β must include alpha particles and impurities

TABLE II INTOR REFERENCE POINT PARAMETERS

E_R	17.6		MeV
Plasma Area/Chamber Area	0.84		
q_I	2.1		
T_n	10		keV
$\bar{n}$	1.4×10^{20}		m^{-3}
e	1.6		
R	5.2		m
a	1.2		m
β_I	2.6		
t	3		m
B_o	5.5		T
$<\beta>$	5.6		%
x	1.00		
f_I	0.33		
B_1	11.4		T
I_p	6.4		MA
τ_E	1.6		s
ν_n, ν_T	1,1	0.2,2	
F	1.03	0.9	
f_n	0.75	0.73	
β^*	5.00	5.11	%
β^*_{JET}	9.03	9.23	%
P_T	672	614	MW_{th}
P_w	2.04	1.86	MW/m^2
P_C	1.72	1.57	MW/m^2
P_n	1.38	1.26	MW/m^2

so that the values of both parameters are consistent with those quoted in reference 2. This practice is not continued here and values of β^* in the main text are based on fuel density only and should be multiplied by 1.5 (i.e $1/f_I$) before comparing them with values reported for INTOR [2]. The other parameters in the second section of Table II are obtained using the equations of Table I.

The final section of Table II contains additional parameters derived for two types of density and temperature profiles: parabolic density and temperature, and flat density with peaked temperature. The value of F is specified in Appendix A, and f_n is defined in Appendix B. The plasma surface power flux, P_w, and chamber wall power flux, P_c, are derived for INTOR by assuming that 17.6 MeV is emitted from the plasma per fusion event, i.e. that the plasma is in thermal equilibrium at the operating temperature. The neutron wall loading is calculated directly from the chamber wall power flux. Throughout this report P_c is loosely referred to as the "wall loading".

The flat density peaked temperature example of Table II comes closest to quoted INTOR parameters. This is misleading, however, since small changes in dimensions and fields will make the parabolic profile example conform. More importantly, flat density and peaked temperature profiles occur in experiments [12] and are therefore assumed to be present in INTOR [13] especially when fuelling and burn control are considered. These profiles are therefore treated here as most closely representing INTOR physics.

The INTOR design point lies on a solution curve to equation (B) of Table I, where the same "physics" parameters as in INTOR, summarised in Table III, and the additional assumptions of P_T = 614 MW_{th}, P_c = 1.57 MW/m^2, c = 2.5 x 10^5 £/m^3 and t = 3m, have been taken. The solution curve is shown in figure 1. The measure of cost, K, is plotted against peak toroidal field, B_1, and as previously explained, a double-valued solution curve is produced. Figure 2 shows that the solid part of the curve includes those devices with central solenoid field $B_c < 10$ T which have high aspect ratio and hence low reactor β^*. The broken part of the curve describes designs with central solenoid

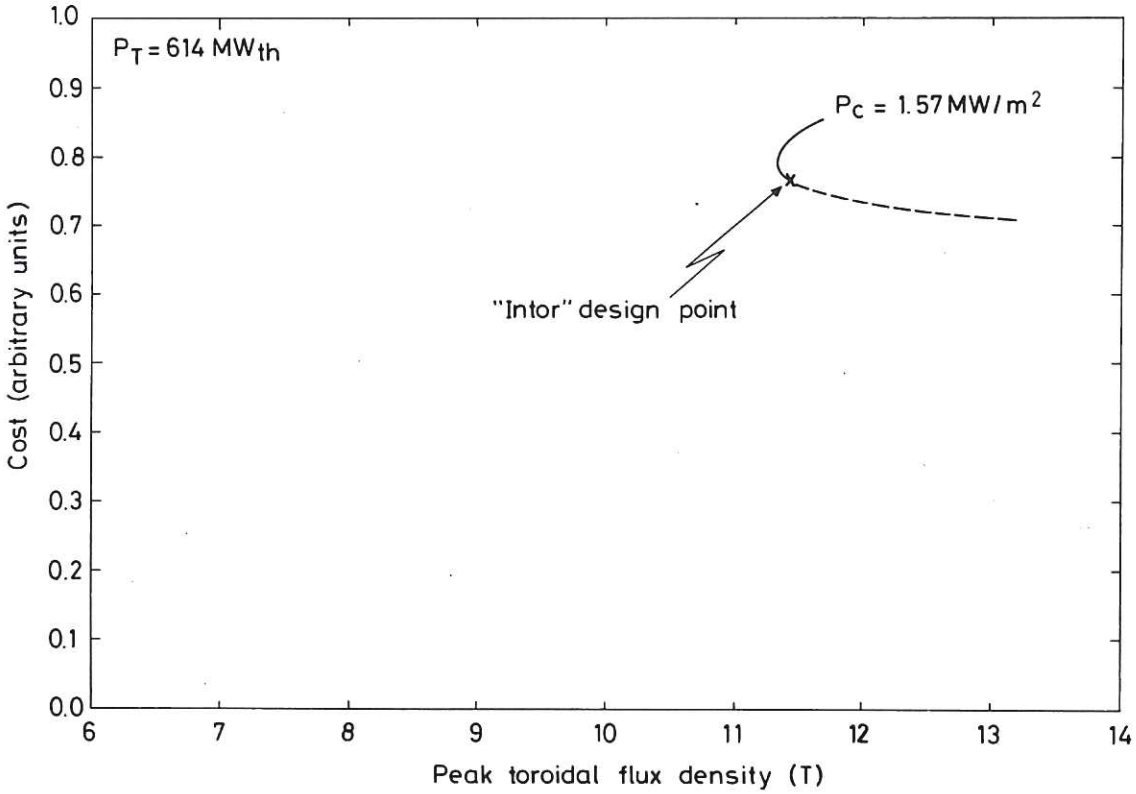

Fig.1 Model solution curve under INTOR physics assumptions.

TABLE III INTOR "PHYSICS" PARAMETERS

E_R	17.6	MeV
Plasma Area/Chamber Area	0.84	
F		0.9
q_I	2.1	
f_n	0.73	
T_n	10.0	keV
β^*_{JET}	9.23	%
e		1.6
x		1.0
ν_n	0.2	
ν_T	2.0	

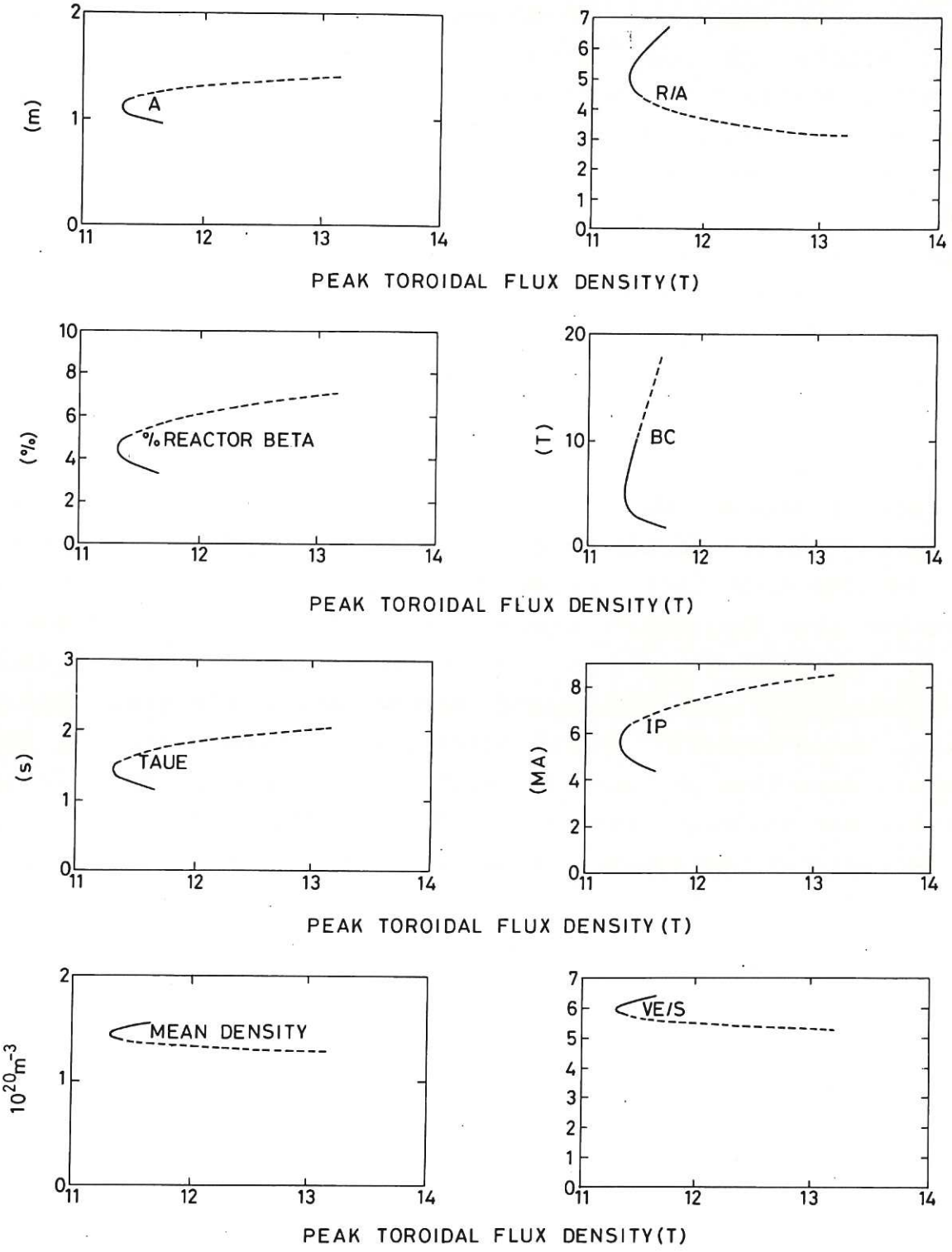

Fig.2 Variation of parameters along solution curve of Figure 1.

field > 10 T and tight aspect ratio with a correspondingly high β^*. The cross on the curves is the 10 T solenoid field point which, to the accuracy of this calculation, is indistinguishable from the INTOR design point. The broken curve stops when the solenoid field becomes infinite. The solid curve stops when "global ignition" becomes impossible, where this condition is defined by integrating both sides of $3nkT/\tau_E < n^2\langle\sigma v\rangle E_\alpha/4$ over the plasma profiles. This condition reduces to a restriction on the maximum major radius for ignition, which from equation 5 of Table I leads to a restriction on the minimum minor radius, for devices of constant power output and wall loading.

Figure 2 also shows that as aspect ratio decreases, mean plasma density falls marginally despite increasing reactor β^*. This occurs because the fall in B_o^2 with decreasing aspect ratio more than cancels out the increase in β^* (see equation 2 in table I). Despite this fall in mean density, energy confinement time increases with decreasing aspect ratio due to its dependence on a^2, as does plasma current. The final curve of figure 2 shows the quotient of the engineered volume and the plasma surface area. The engineered volume thickness is fixed here but this quotient describes the average thickness of the engineered volume attributable to unit area of the first wall, taking account of the geometry of the torus. It is therefore a measure of the mean engineered volume thickness per unit power output (since wall loading is constant along a design curve) of different designs. Since the cost in figure 1 is based on the engineered volume per unit output the minimum cost is obtained where this quotient is lowest.

The cost scaling, under constraints of constant toroidal field and variable wall loading is described in more detail elsewhere [5]. Figure 1 shows, however, that the INTOR design requires close to the minimum peak toroidal flux density under the constraints of plasma physics, power output and wall loading specified.

How well do these constraints satisfy the aims, described in the introduction, of TNS devices such as INTOR? It is too early to tell at present whether the physics described in Table III is a reasonable step beyond JET. The suitability of this physics

for DEMO and CTR devices and the effect of using "better physics" is considered in section 5. From the materials testing viewpoint the wall loading level is above that required but it would take 15 years operation at 25% availability to reach 5 MWy/m^2 total accumulated dose. This calls into question the ability of such a device to satisfy the third aim, of adequately testing and developing the components and technologies required for DEMO.

How can this situation be improved? To produce the design curve of figure 1 the thermal power output of the device was fixed. This is unnecessary for TNS, since only token electricity generation is contemplated, and the only requirements are that the plasma must ignite and that adequate wall loading must be achieved at tolerable field levels. Figure 3 indicates the design space for TNS devices of different P_T but the same wall loading as in INTOR. Note that costs are expressed as total engineered volume costs (i.e. KP_T) and that INTOR physics is retained. With 12 T and 10 T as notional peak tolerable toroidal and central solenoid fields respectively, designs with power output much below that of INTOR cannot ignite without exceeding these limits. Higher thermal power output devices than INTOR ignite readily and require considerably lower fields. The price is a much larger engineered volume and higher cost.

If wall loading is allowed to rise in higher power output devices their cost disadvantage is considerably reduced as the design becomes more compact. This is illustrated in figure 4 for a 1000 MW_{th} design at a number of different wall loadings. The parameters of a 1000 MW_{th} device with the same peak toroidal field as in INTOR, but at the maximum wall loading attainable are shown in the second column of Table IV with INTOR parameters for comparison. This design exhibits a 36% improvement in wall power loadings and doses for materials testing, for a 63% increase in device power output but only a 17% increase in engineered volume cost. This design maximises the wall loading for the given field. A slightly cheaper device, due to increased compactness, can be arrived at by considering only devices with central solenoid fields of 10 T. Figures 3 and 4 show that such designs come close to minimising wall loading for a given field. Typical parameters are shown in column 3 of Table IV.

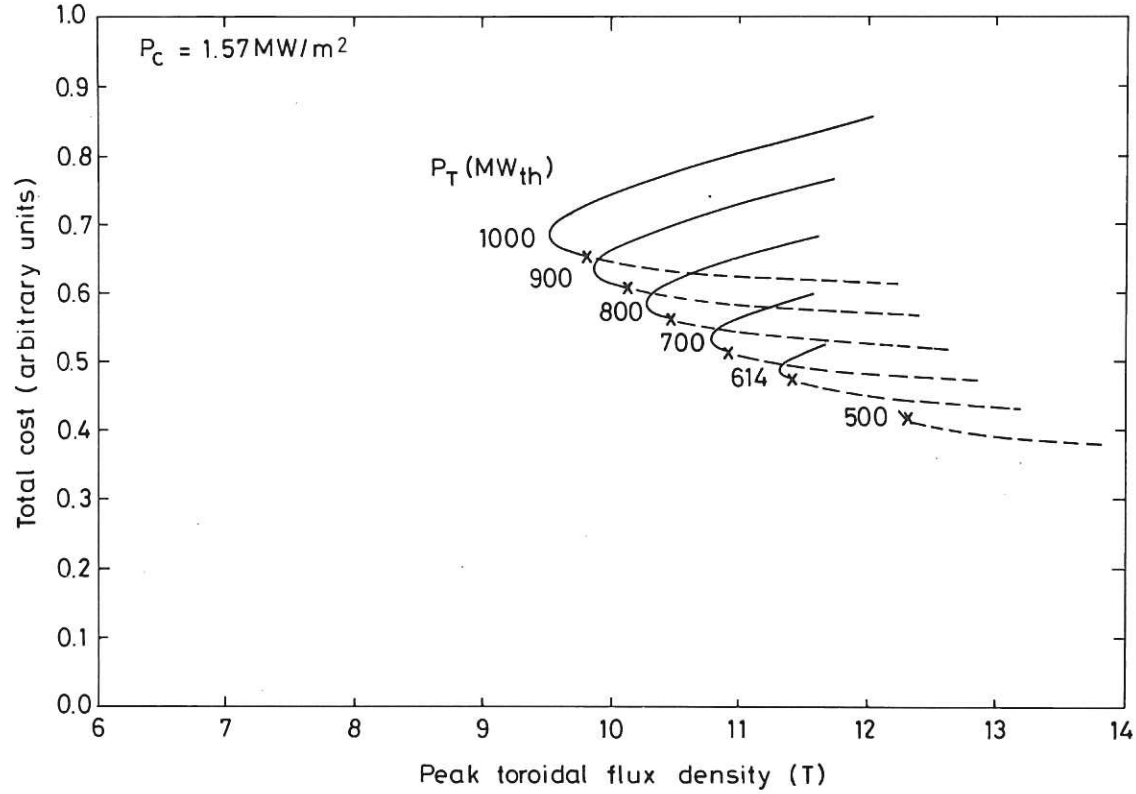

Fig.3 Design curves for INTOR wall loading at various power outputs.

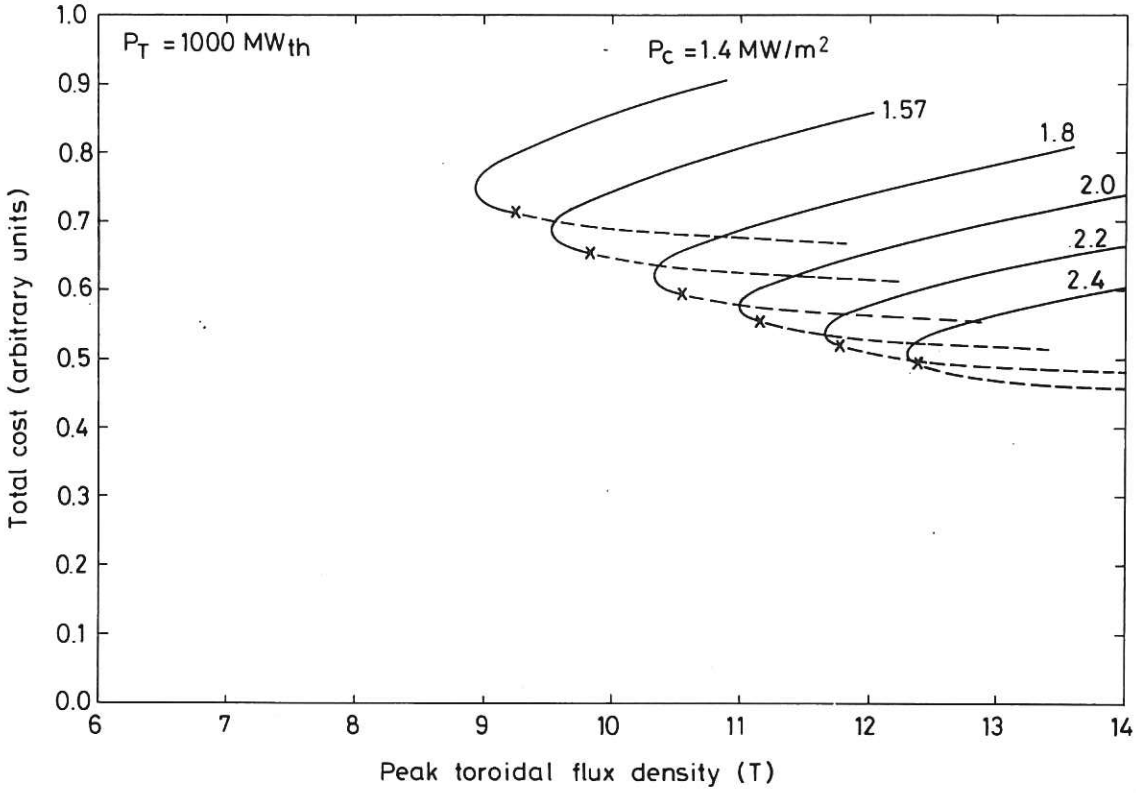

Fig.4 Design curves for a 1 GW$_{th}$ device at various wall loadings.

Instead of improving INTOR parameters to satisfy TNS device aims more readily, the risk associated with only achieving INTOR wall loadings might be accepted and designs contemplated which require lower toroidal field. As an example of this the power loading of the 1000 MW_{th} devices described above have been scaled down, keeping dimensions constant, to achieve the same wall loading as in INTOR. The resulting parameters are shown in columns 4 and 5 of Table IV and the peak toroidal field is reduced by about 7%.

This section illustrates the characteristics of the model of Table I when applied to the study of TNS devices such as INTOR. When applied to DEMO and CTR device aims the variation of parameters and thus the conclusions drawn will be qualitatively similar. The results show that there is considerable flexibility in choosing TNS device parameters but that higher costs are usually incurred when moving away from the INTOR design point. To decide whether the increased cost of TNS devices operating at low field is worthwhile requires an understanding of the field requirements of DEMO and CTR devices. This is dealt with in the next section.

TABLE IV - TNS PARAMETER OPTIONS

	INTOR	HIGH WALL LOADING		LOW PEAK FIELD		
P_T	614	1000		735	753	MW_{th}
P_c	1.57	2.14	2.08	1.57		MW/m^2
B_1	11.4	11.4		10.6	10.7	T
KP_T	0.47	0.55	0.54	0.55	0.54	Arbitrary
R	5.20	6.00	5.53	6.00	5.50	m
a	1.20	1.24	1.39	1.24	1.39	m
β_I	2.6	2.9	2.4	2.9	2.4	
B_o	5.5	6.2	5.4	5.7	5.1	T
β^*	5.1	4.6	5.5	4.6	5.6	%
$\bar{n}$	1.4	1.6	1.5	1.4	1.3	10^{20} m^{-3}
τ_E	1.6	2.0	2.3	1.7	2.0	s
I_p	6.4	6.8	8.0	6.3	7.6	MA
B_c	10.0	4.4	10.0	4.1	10.0	T

4. DEMO AND CTR DESIGNS

TNS devices are unlikely to be capable of producing net power output even if their thermal output were converted to electricity. To keep capital costs and technical difficulty to a minimum, heat removal from the blanket takes place at low temperature and is not even converted to electricity to run the reactor. However, DEMO and CTR devices must produce net electrical power, though the DEMO device would be permitted to be less efficient and cost effective than a CTR. Possible DEMO and CTR specifications might thus be as given in the first section of Table V. The difficulty of capturing all the fusion energy as high grade heat in DEMO is reflected in the rather low thermal efficiency assumed. For CTR, however, efficiency will be maximised. Since the circulating power in INTOR is ~ 200 MW_e and that for DEMO and CTR must therefore be higher, the net electricity production from such devices might be in the region of 300 MW_e and 800 MW_e respectively.

To minimise total cost, DEMO will be as small as is possible while satisfying the design aims indicated in the introduction. Ensuring an adequate tritium breeding margin allowing for hold-up in untried systems will require the careful use of multipliers and enriched lithium in the blanket to improve the neutron economy. Overall energy multiplication of fusion neutron energy in the blanket cannot therefore be guaranteed and the energy available per fusion event may not exceed 17.6 MeV. This value is used here for DEMO. The design curves are only marginally affected by assuming a higher value, the resulting increased power output at a given wall loading being compensated by a minimal (< 4%) reduction in peak field. For a CTR the blanket design must be improved to make the best energetic use of the neutrons generated. A figure of 20 MeV/reaction has been used in previous studies [5] and this will therefore be used here. Since in calculations using this model P_c is obtained by dividing thermal power output by chamber area, the first wall power flux is 17.6/20 = 88% of the values quoted here for CTR.

Typical design curve families for DEMO and CTR are shown in figures 5 and 6, showing cost per unit power output for the purposes of comparison. These results have been derived under

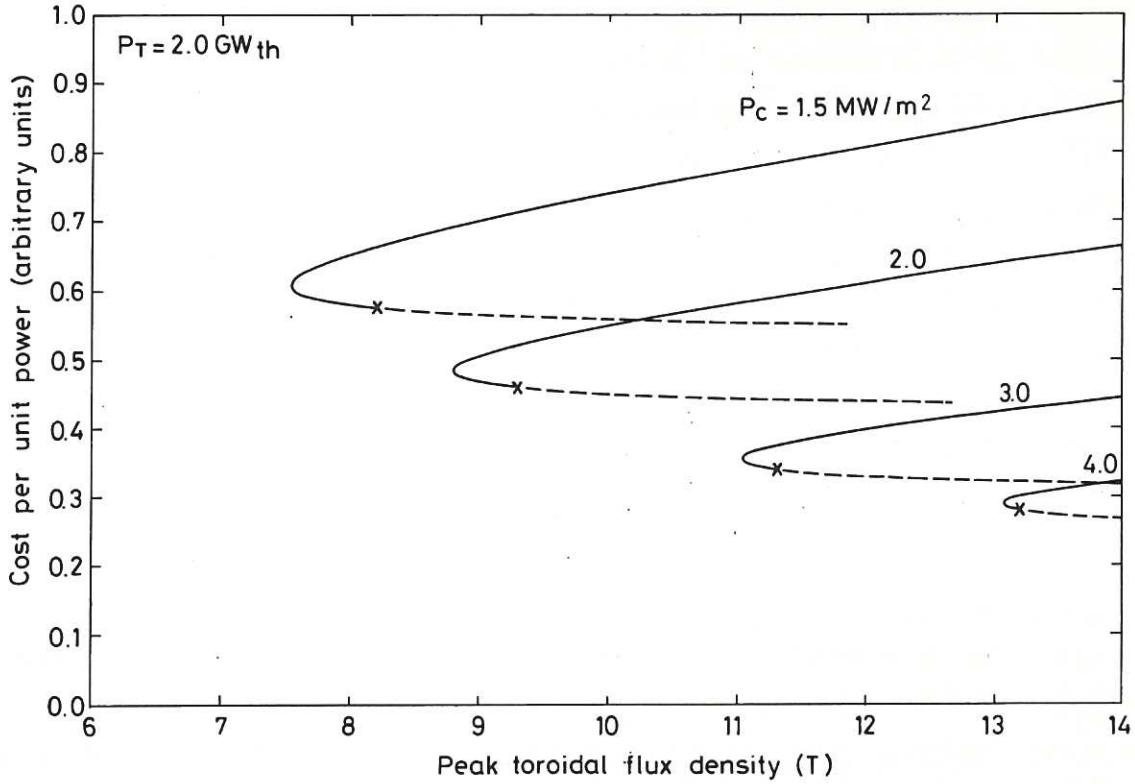

Fig.5 Design curves for a DEMO reactor.

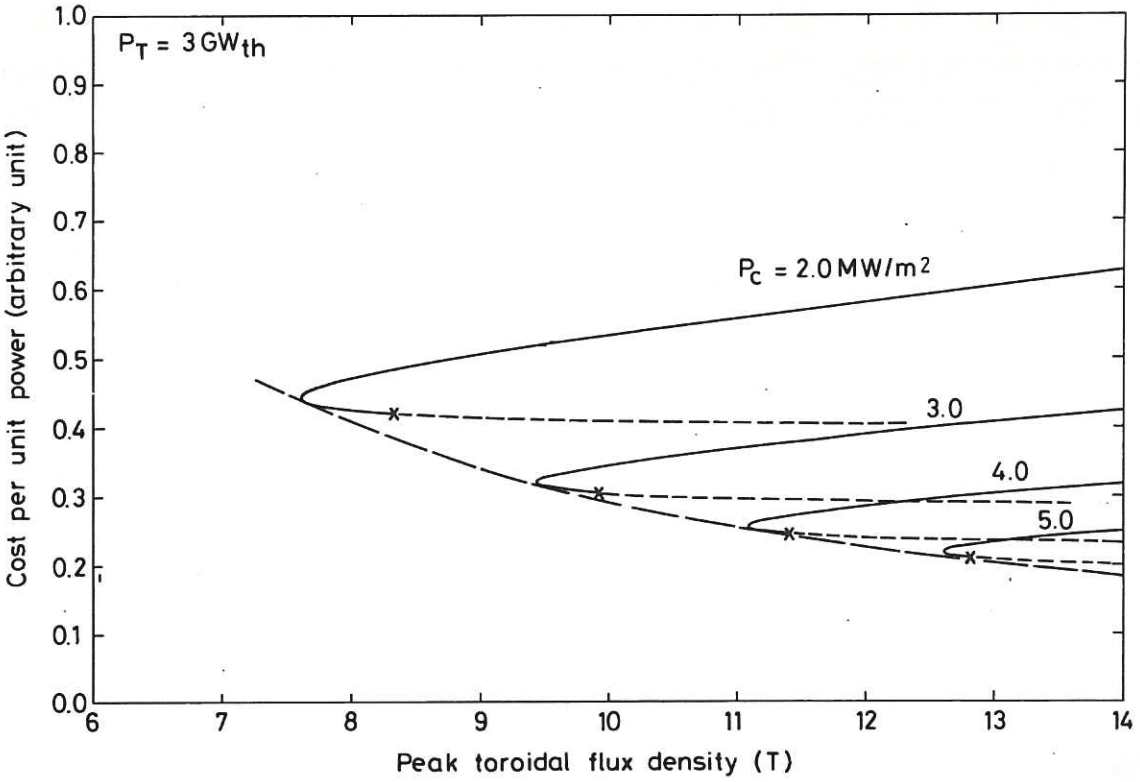

Fig.6 Design curves for a CTR.

the same physics assumptions as used in INTOR (see Table III) and assuming an engineered volume thickness t of 3 m. Comparison with figures 1, 3 and 4 indicates that the minimum magnetic field for a given wall loading has been much reduced by considering devices of higher power output. Even in DEMO, wall loadings similar to those shown for the high wall loading TNS device in Table IV can be produced for fields of only 9T compared to the 11.5 T required there. On the other hand fields of 11-12 T in DEMO would allow the wall loading to be doubled over the INTOR value if this were to prove to be advantageous.

Figure 6 indicates the incentive for attaining a given wall loading. From the minimum cost envelope of the design curves, it is apparent that increased wall loading, with the consequent increase in toroidal field in a constant power output device, produces a diminishing cost saving as field is increased. For instance, only a cost saving of 15% is made by going from 4 to 5 MW/m^2 compared to a saving of 28% in going from 2 - 3 MW/m^2. Irrespective of the field required, therefore, there is no incentive to exceeding 4 - 5 MW/m^2, since much higher wall loadings would be required to significantly reduce the cost. Since these cost savings are only those associated with the engineered volume, the percentage saving will be considerably reduced when total reactor costs are considered. Thus fields of 11 - 12 T and wall loadings of about 4 MW/m^2 appear to be near the maximum necessary for CTR designs.

This conclusion assumes that toroidal field coil costs scale only with coil volume. Even when this cost scaling is replaced with more realistic modelling the same conclusion persists. The minimum cost envelope curves of CTR designs are illustrated in figure 7 along with the reference scaling for two scalings with field. The first of these assumes cost scales with B_1^2 from that cost (based on the coil volume) at 8 T. The second scaling [8] incorporates the different cost scalings of the individual parts of the toroidal field coil system and support structure. Both these scalings increase the cost of higher field systems over the reference system. However, since the toroidal field coil system makes up only about 25% of the engineered volume, there is only a weak minimum in cost at high field. Much stronger scalings would

be required to significantly alter the conclusions drawn from a simple volumetric costing, and this bears out the assumption made in the model of Table I.

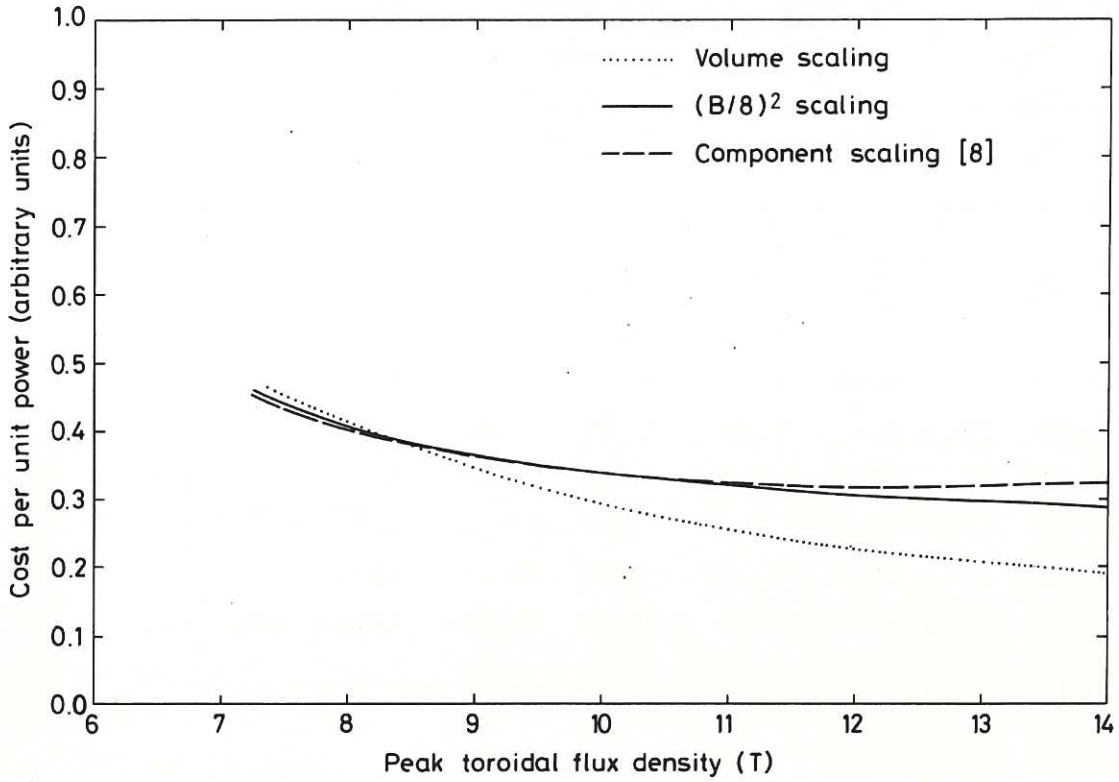

Fig.7 The effect of different toroidal field coil cost scalings on the design envelope of the CTR.

The parameters of DEMO and CTR can be determined on the basis of a number of different assumptions about TNS. If high fields are developed for TNS designs and used for DEMO and CTR, then the reactor parameters shown in columns 1 and 3 of Table V are obtained. (A central solenoid field of 10 T has been retained for consistency, though 8 T parameters do not differ greatly.) These parameters should be compared to column 3 of Table IV. Alternatively, if only comparatively low fields are developed for TNS designs and used on DEMO and CTR, the parameters in columns 2 and 4 of Table V result. These should be compared to column 5 of Table IV. For both DEMO and CTR the cost parameter K indicates that there is only a small penalty associated with not developing high field systems along the route to a CTR.

TABLE V - DEMO & CTR PARAMETER OPTIONS

	DEMO		CTR		
P_T	2000		3000		MW_{th}
η_{TH}	30		40		%
E_R	17.6		20.0		MeV
t	3.0		3.0		m
B_l	11.4	10.7	11.4	10.7	T
P_c	3.1	2.7	4.0	3.5	MW/m^2
B_c	10.0	10.0	10.0	10.0	T
R	6.06	6.28	6.33	6.57	m
a	1.71	1.89	1.89	2.08	m
β^*	6.3	6.7	6.6	7.0	%
$\bar{n}$	1.6	1.5	1.7	1.5	$10^{20}\ m^{-3}$
I_p	11.0	11.9	12.7	13.5	MA
K	0.33	0.37	0.25	0.27	Arbitrary

5. RESULT SENSITIVITY

These results are sensitive to the physics and engineering assumptions on which they are based.

Although profiles of density and temperature can have an effect on the results, the more uncertain physics parameters at this stage are the pressure ratios and their scaling, expressed through the choice of the values of β^*_{JET} and x. For illustrative purposes the change in the envelope of the DEMO design curves is shown in figure 8 as a function of x along with the locus of the tangent points to the design curves at specific wall loadings. Equation 4 of table I shows that increasing the scaling index of poloidal beta increases the reactor β^* value for a given β^*_{JET} at fixed dimensions. This results in a reduction in the field required for a given output power. Also shown in figure 8 are the horizontal axes to be used at different values of β^*_{JET}. These axes can be applied to all the other graphs in this report, since $B_l \propto (\beta^*_{JET})^{\frac{1}{2}}$. The same scaling applies to the design

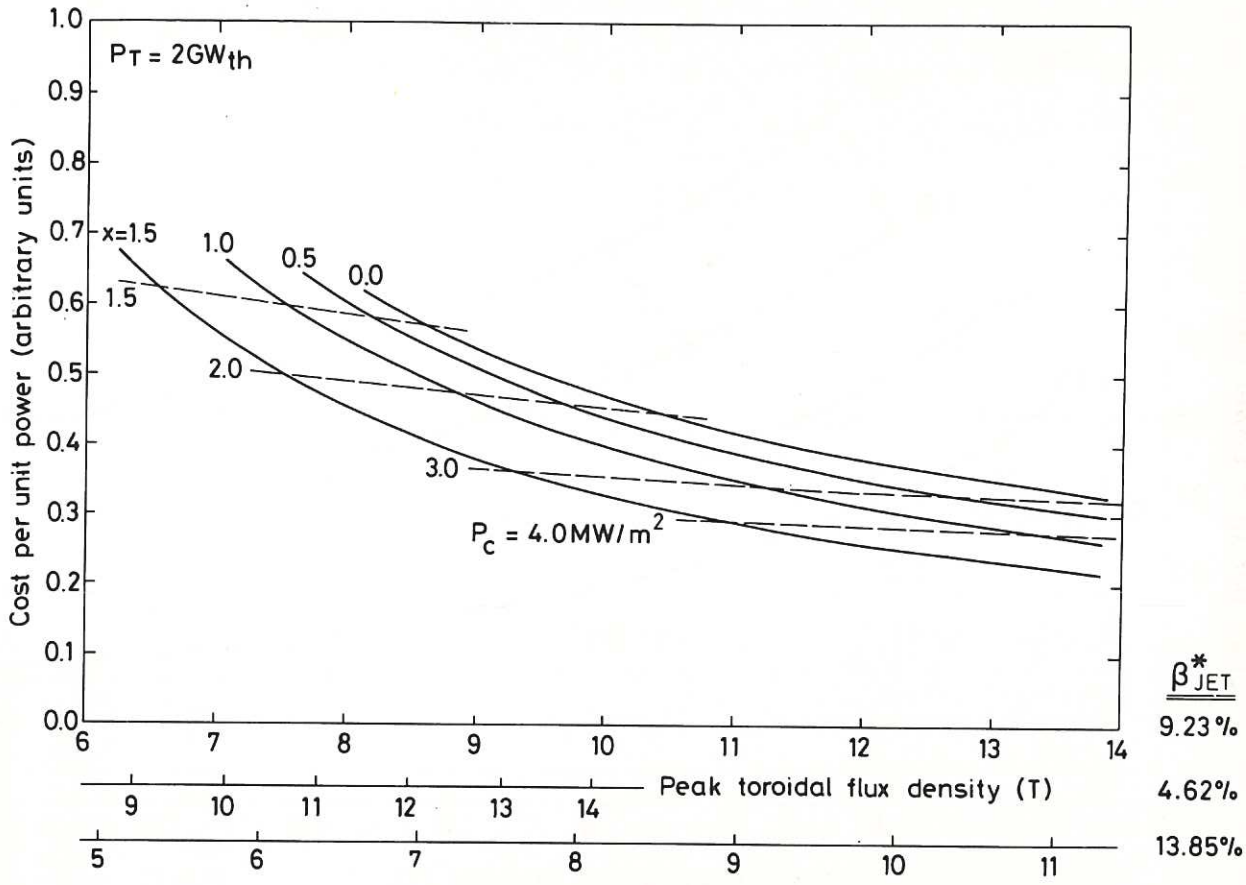

Fig.8 Variation of DEMO design points with value of β^*_{JET} and poloidal beta scaling index x.

points quoted in the tables. Any conclusions about the need for fields of a particular value must therefore be tempered by these physics uncertainties. Results from JET are essential to give guidance in this area.

The major engineering assumption made so far has been the thickness of the blanket, shield and coils. Up to this point a value of 3m has been used, close to that applying to INTOR. In INTOR, however, no tritium breeding takes place on the inboard side of the plasma. In DEMO and CTR designs more space may be needed for this function and to reach suitable coolant temperatures for efficient electricity generation. Figure 9, therefore, shows how, for example, the design curve envelopes for DEMO change with varying values of t. Once again the locus of

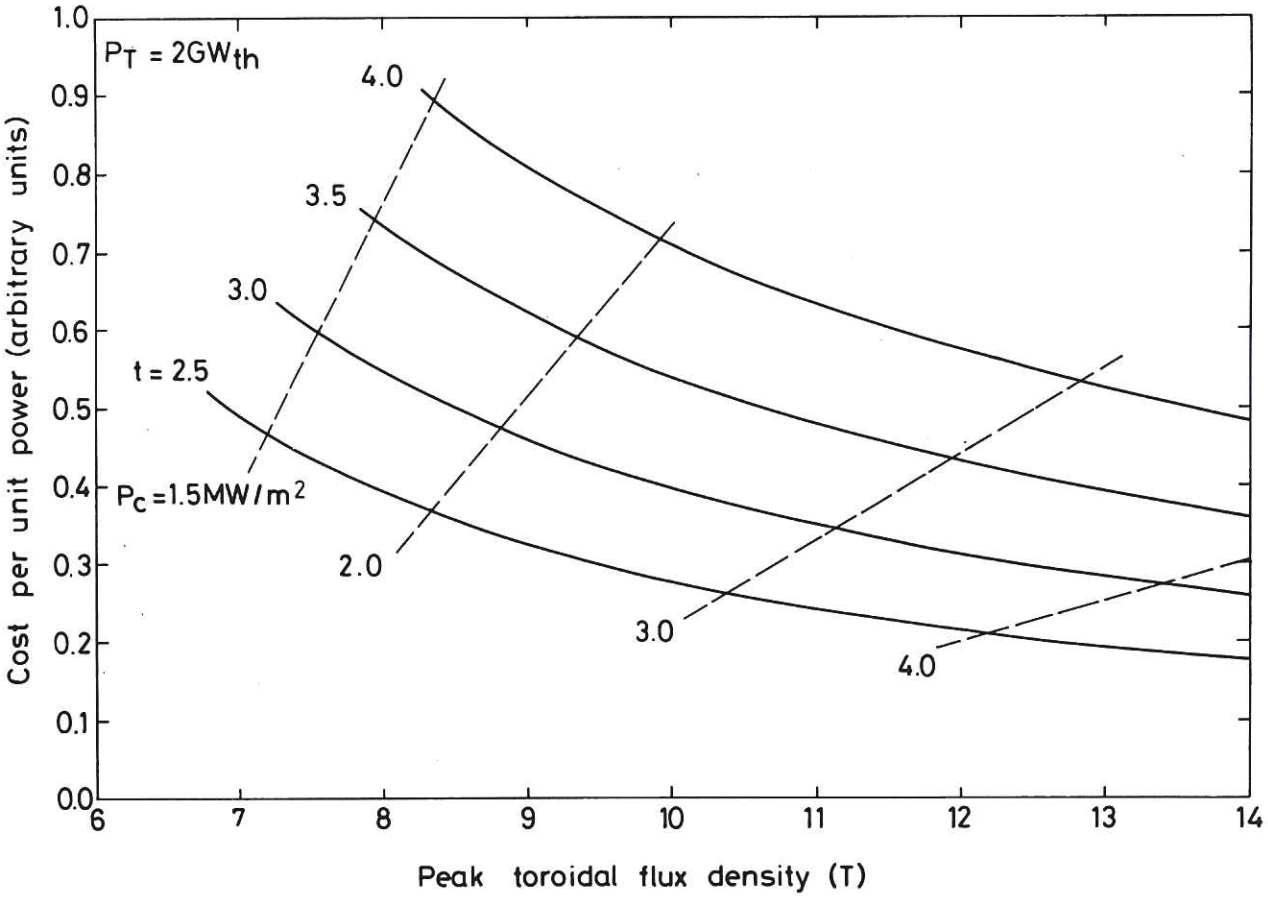

Fig.9 Variation of DEMO designs points with blanket/shield/coil thickness, t.

the tangent points of the various wall loading design curves are shown. Since the cost defined here depends entirely on the engineered volume, which in turn depends strongly on t, the cost increases rapidly as t increases, unless a corresponding increase in wall loading is made. This 'compensation' can only be achieved by using a much higher peak toroidal field, which in this model is sensitive to t/2, the assumed inboard blanket/shield thickness.

Thus, the larger the value of t, the greater is the incentive to move to high fields. There are clear benefits apparent in making t as small as possible and this is a strong incentive for carrying out detailed blanket and shield designs. Similar results apply to INTOR showing that blanket and shield designs with t much greater than 3 m cannot be tested out in position on the inboard side of the plasma unless the wall

loading of such a device is decreased or the power output increased - otherwise the field value required will rapidly become too large (beyond 12T).

However, in section 3, a TNS design with the same wall loading as in INTOR but higher power output and consequently lower peak field was developed (Table IV, column 5). If, instead of reducing peak field, the INTOR field level had been retained, then an increased blanket and shield thickness could be obtained in a device of the same wall loading as INTOR, with parameters shown in Table VI. To increase t by 0.5 m involves a 50% increase in the total engineered volume cost over that of INTOR. When compared to the low-field device of Table IV at the same thermal power output level, this is still a 30% cost increase. Further increases in power output allow t to become larger still while still maintaining peak field and wall loading at INTOR values. However the cost will be even higher than the above.

TABLE VI DESIGN PARAMETERS WITH INTOR PHYSICS & FIELDS AND MAXIMISED INBOARD BLANKET/SHIELD THICKNESS

	TNS	DEMO	CTR	
P_T	753	2000	3000	MW_{th}
P_c	1.57	2.7	3.5	MW/m^2
B_l	11.4	11.4	11.4	T
B_c	10.0	10.0	10.0	T
R	5.92	6.81	7.20	m
a	1.29	1.73	1.90	m
β^*	4.8	5.6	5.8	%
$\bar{n}$	1.3	1.5	1.6	$10^{20}\ m^{-3}$
I_p	6.6	10.2	11.5	MA
K	0.70*	0.50	0.39	Arbitrary
t	3.50	3.65	3.76	m

* KP_T

For DEMO and CTR the same use can be made of the development of INTOR field levels to maximise the available inboard blanket/shield space. The parameters of such devices, shown in Table VI should be compared with the low field designs of Table V. The engineered volume costs per unit output are increased by 35% and 45% respectively over the low field DEMO and CTR designs at the same wall loading. Of course, a compromise between the device parameters in Tables V and VI may be beneficial.

6. SUMMARY AND CONCLUSIONS

The application of a simple model inter-relating physical and technological system parameters and costs, to determine the incentive for acquiring the ability to use high field magnets in future tokamak devices, has been described. The strength of the incentive has been placed in context by relating the results to the future attainments of the JET experiment and the physics expected to prevail in INTOR. The sensitivity of the results to this latter assumption has been examined.

The model shows that for the wall loading and power output requirements of INTOR, the present INTOR design point occurs close to the minimum peak toroidal field attainable. Without increasing the thermal power output there is little room for improving the wall loading in INTOR without using fields above 12 T. However, with the same physics assumptions but with the thermal power output increased to 1000 MW_{th} for example, a 36% increase in wall loading can be obtained for only a 17% increase in the total cost of the engineered volume. Alternatively, this increase in cost would also be obtained for a device with a 7% lower peak field and the original wall loading of INTOR. It is possible for a 1000 MW_{th} device to reach the INTOR wall loading level with peak fields under 10 T (figure 3) but the total cost of the engineered volume would exceed that of the present INTOR design by 50%. This might be an acceptable alternative to high field coil development if the effect on the cost of DEMO and CTR's proved to be negligible.

For DEMO and CTR devices, fields certainly no higher than required in INTOR are necessary to satisfy the economic aims described in the introduction, since the cost per unit output of

a CTR improves only marginally above 4 MW/m^2. Peak fields no higher than 10.7 T appear to be required to reduce CTR engineered volume costs to within 10% of the cost obtained for a CTR with the higher fields of 11.4 T required for INTOR (Table V). Furthermore, only an engineered volume cost increase of 20% is predicted for CTR's if the peak field remains below 10 T (figure 6).

Are there any advantages for DEMO and CTR in developing field levels to that needed for INTOR or even beyond? One possible advantage is that the increased field could be used to provide room for the thicker blankets and shields that may be needed for high temperature tritium breeding operation, without degrading the wall loading level attained. Unfortunately, much higher fields are needed to maintain engineered volume costs per unit power at a tolerable level even with a modest increase in blanket/shield thickness (figure 9). Thus there will always be the greatest pressure to minimise the inboard blanket/shield thickness to reduce costs generally, and this may make the acceptance of a marginally reduced wall loading preferable to the development of higher field systems.

Another possible advantage of high field coil system development is that underachievement of β levels or unfavourable scaling of β to reactor level could be counteracted. However, a more optimistic viewpoint is that β levels will rise from presently expected values as the understanding of plasma physics increases. Since the shape of the cost curves indicates diminishing benefits in devices of increasingly high wall loading, increases in β would be made use of by decreasing the peak toroidal field.

This study therefore raises three questions which must be answered before the incentive for high field can be clearly established:

(1) How high can β^* be in JET?
(2) How does poloidal β scale with aspect ratio?
(3) How thin can a high temperature tritium breeding blanket be on the inboard side of the plasma?

With the present uncertainty in these parameters it is not possible to confirm or deny with complete confidence the need for peak toroidal fields as high as in INTOR (11.4 T). With physics assumptions at present considered reasonable, however, fields under 11 T appear quite adequate as long as thin, high temperature tritium breeding blanket systems can be designed. This makes question (3) above the most critical at the moment. If tokamak reactor physics exceeds present expectations by as little as 30% on β^* (figure 8), then peak fields below 10 T may be sufficient, and considerable magnet development costs may be saved at the expense of a potentially minimal cost increase in the final fusion device.

In answer to the question raised in the introduction, therefore, the studies reported here indicate that there is little financial risk, in the long term, associated with not developing high field magnets (e.g, beyond 10 T). In the shorter term, however, for next-step devices to satisfy their aim, fields of about 10 T will be required. If attainable levels of β^* (9.2% needed in JET) or inboard blanket/shield/etc thickness (1.5 m) fall below present expectations, the incentive to ultimately develop higher fields coils is strengthened. Even then, the incentive is weak if the shortfall is modest (10 - 20%). Conversely if high field (e.g. 12 T) magnets were available for next step devices, considerably higher wall loading devices with their improved materials testing capability could be constructed at an earlier stage than with a "low-field" development programme. However, as stated, the ultimate savings in cost per unit power for a commercial design would be small.

REFERENCES

[1] Carruthers R., Unconventional Approaches to Fusion (ed. B. Brunelli and G.G. Leotta), Plenum Press (1982) pp39-45

[2] INTOR Group, INTOR Phase I Executive Summary, EUR-FU-BRU/XII-132/82/EDV1 (1982)

[3] STARFIRE/DEMO Team, Argonne National Laboratory Report ANL/FPP/TM-154 (March 1982)

[4] Knobloch A.F., Max Plank Institut fur Plasmaphysik Report IPP 4/144 (1976)

[5] Spears W.R., Wesson J.A., Nucl. Fus. 20(12), 1525-1532 (1980)

[6] Hollis A.A., Harwell Report AERE-R9933 (1981)

[7] Fraas, A.P., Oak Ridge National Laboratory, ORNL-TM-4080 (1974)

[8] Cooke, P.I.H., Scaling of Superconducting Toroidal Field Coil Costs and Implications for Tokamak Reactor Design, to be published in Proc. 10th Symposium on Engineering Problems of Fusion Research, Philadelphia, December 1983

[9] Abdou, M.A. et al., Fusion Reactor Design Concepts Proc. IAEA Workshop, Madison (1977) p673-699

[10] Flanagan C.A., Steiner D., Smith G.E. et al, FED Device Design Description, ORNL/TM-7948/VI (1981) p2-86 et seq.

[11] Sykes A., Beta Limits in Tokamaks, submitted to Controlled Fusion and Plasma Physics, Proc. 11th European Conference, Aachen, September 1983

[12] Rawls J.M., United States Dept. of Energy Report DOE/ER-0034 (1979)

[13] Duchs D.F., Plasma Physics for Thermonuclear Fusion Reactors, ed. G. Casini, Harwood Academic Publishers GmbH EUR 7647 EN, pp445-491 (1981)

Appendix A - REACTION RATE CORRECTION FACTOR, F

To correct the reaction rate for different plasma density and temperature distributions the profile factor $F(\nu_n, \nu_T)$ was introduced in equation (A) of Table I. Typical values of F at a density weighted mean temperature of 10 keV are shown in the figure below.

From Table I:

$$F = \frac{\int n^2 \langle \sigma v \rangle \, dV}{\left[\frac{\langle \sigma v \rangle}{k^2 T^2}\right]_{T_n} \int n^2 k^2 T^2 dV}$$

where n, T and hence $\langle \sigma v \rangle$ are functions of position and $[\ ]_{T_n}$ means "evaluated at T_n".

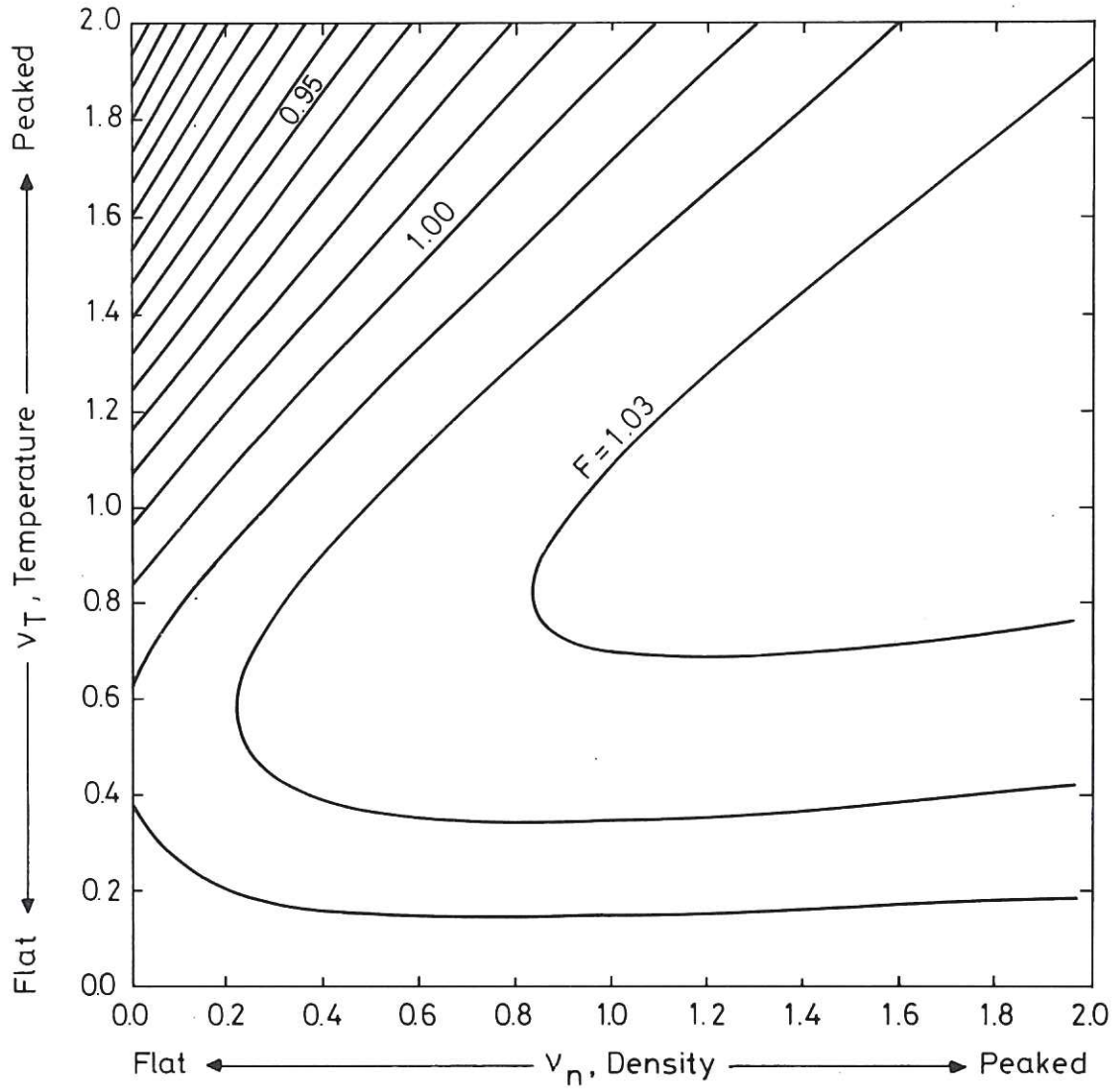

Fig.A1 The profile factor F at 10keV.

Appendix B - CONSISTENT INTOR PARAMETER DERIVATION

The INTOR parameters listed in Table II are mainly obtained directly from reference 2 where they are either stated explicitly or can be derived from the design parameters. However, some INTOR parameters most useful here, are not stated explicitly. Also, the INTOR parameters of reference 2 are not necessarily self-consistent, being the broad average of parameters derived by the different INTOR design teams at the end of Phase Zero of INTOR in 1981. To have a consistent set of parameters for the INTOR design point, certain additional assumptions and parameter choices must be made and these are described below.

An initial assumption is that electron temperature and density profiles are given by:

$$n_e = n_{eo} (1 - r^2/a^2)^{\nu_n}; \quad T_e = T_{eo} (1 - r^2/a^2)^{\nu_T}$$

For ions, a constant fraction f_I is allowed for alpha particles and impurities and all the ion profiles are treated as being proportional to the electron profile (i.e. same value of ν_n as for electrons). Ion temperature is equated to electron temperature. In the above the values of density and temperatures at r and a are treated as flux surface averaged values, and integration over the plasma volume is therefore achieved by treating an elementary volume as

$$dV = 4\pi^2 R e r dr$$

Average pressures, densities and temperatures are defined by:

$$\langle p \rangle = \frac{\int 2 n_e k T_e dV}{\int dV} = 2\, n_{eo} k T_{eo} \frac{1}{(\nu_n + \nu_T + 1)}$$

$$\langle n_f \rangle = (1 - f_I) \frac{\int n_e dV}{\int dV} = (1 - f_I) \frac{n_{eo}}{(\nu_n + 1)}$$

$$\langle T \rangle = T_n = \frac{\int n_e\, T_e\, dV}{\int dV} = T_{eo} \frac{(\nu_n + 1)}{(\nu_n + \nu_T + 1)}$$

where n_f is the density of fuel ions.

Poloidal and toroidal beta are defined by:

$$\beta_I = \frac{4\pi^2 (1+e^2) a^2 \langle p \rangle}{\mu_o I_p^2} \quad ; \quad \langle \beta \rangle = \frac{2\mu_o \langle p \rangle}{B_o^2}$$

The basic INTOR parameters quoted in reference 2 are:

$\langle n_f \rangle = 1.4 \times 10^{20}$ m^{-3}
$\langle T \rangle = 10$ keV
$\langle \beta \rangle = 5.6\%$
$\beta_I = 2.6$
$B_o = 5.5$ T
$a = 1.2$ m $R = 5.2$ m $e = 1.6$

If parabolic profiles are assumed for density and temperature, i.e. if $\nu_n = \nu_T = 1$, the following parameters may be derived:

$\langle p \rangle = 6.7 \times 10^5$ N/m^2
$I_p = 6.5$ MA
$T_{eo} = 15$ keV
$n_{eo} = 4.2 \times 10^{20}$ m^{-3}
$f_I = 0.33$

Now since n_{fo} is assumed to be $(1 - f_I) n_{eo}$, $n_{fo} = 2.8 \times 10^{20}$ m^{-3}.

The mean square pressure:

$$\langle p^2 \rangle = 4 n_{eo}^2 k^2 T_{eo}^2 \cdot \frac{1}{(2\nu_n + 2\nu_T + 1)}$$

and therefore

$$\beta^* = \frac{2\mu_o \sqrt{\langle p^2 \rangle}}{B_o^2}$$

is about 7.5%. From appendix A, F = 1.031 so equation (A) of table I gives a thermal power output of 672 MW_{th}, assuming that the fuel β^* is 2/3 of the total β^* based on the above value of f_I. This power output is higher than that quoted in reference 2(620 MW_{th}) so the self consistent wall loading must also be

greater. The wall loading value quoted in Table II is equivalent to a chamber wall neutron wall loading of 1.37 MW/m^2 compared with 1.3 MW/m^2 in reference 2. These discrepancies are not unexpected at this stage since values in reference 2 are given only to two significant figures. Since power output scales with B^4, R, a^2 and β^{*2} small inconsistencies (~ 1%) can easily accumulate.

With these self consistent parameters specified the other parameters in Table II i.e. β^*_{JET}, B_l, I_p and τ_E can be calculated from the equations of table I. The factor f_n is merely used to obtain mean density from β^* using T_n as the equivalent temperature, and is therefore profile dependent. Thus

$$\bar{n} = f_n \frac{\beta^* B_o^2}{4\mu_o k T_n}$$

and therefore

$$f_n = \frac{(2\nu_n + 2\nu_T + 1)^{\frac{1}{2}}}{(\nu_n + \nu_T + 1)}$$

What happens if a peaked temperature and flat density profile (a more realistic situation) are chosen, i.e. ν_n = 0.2, ν_T = 2 ? As above, the following parameters can be derived:

$$\begin{aligned} \langle p \rangle &= 6.7 \times 10^5 \ N/m^2 \\ \langle I_p \rangle &= 6.5 \ MA \\ T_{eo} &= 26.67 \ keV \\ n_{eo} &= 2.51 \times 10^{20} \\ f_I &= 0.33 \\ \sqrt{\langle p^2 \rangle} &= 9.23 \times 10^5 \ N/m^2 \\ \beta^* &= 7.67\% \end{aligned}$$

Appendix A gives F = 0.9 and therefore equation (A) of table I gives 614 MW_{th}, which is close to the value quoted in reference 2.

From the above it is apparent that the choice of profile shape can have a significant effect on certain reactor parameters, particularly power levels. (In fact, thermal power varies between 350 and 1025 MW_e as ν_n and ν_T vary between 0 and 2. This is shown in figure B1.) The peaked temperature, flat

density profile solution approximates to quoted INTOR parameters quite well. Nowhere in the INTOR reports, however, is a definitive profile stated, and the value of the alpha particle and impurity fraction, f_I, of 1/3 is also not discussed. For this study, the peaked temperature, flat density profiles have been considered to typify INTOR physics assumptions.

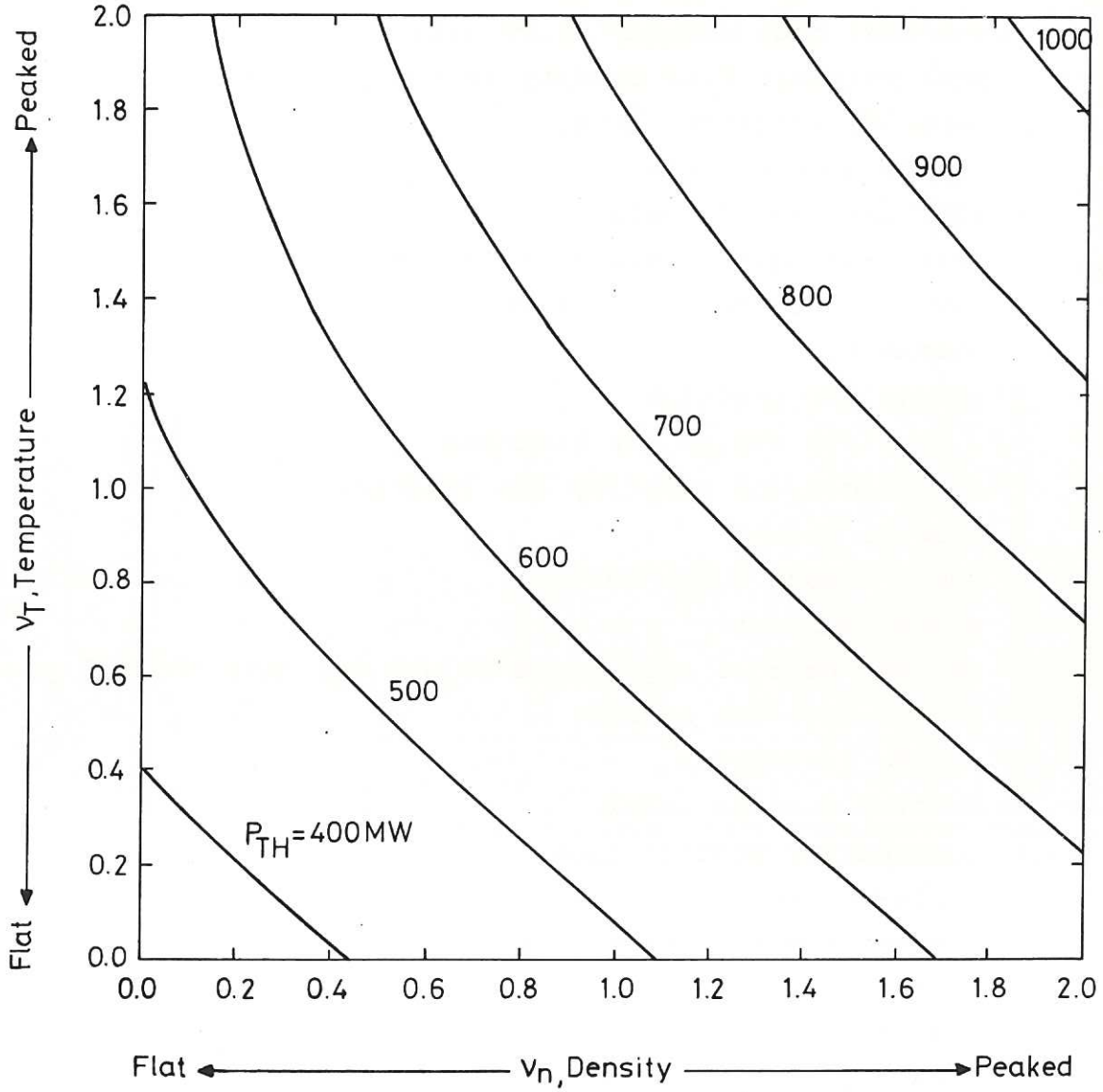

Fig.B1 The effect of density and temperature profile scaling factors on power output for R = 5.2m, a = 1.2m, e = 1.6, E_R = 17.6MeV, $\bar{n}$ = 1.4 X 10^{20} m^{-3}, T_n = 10keV (i.e. INTOR).

Glossary

a	plasma minor radius (minimum)
B_o	toroidal flux density at R
B_1	toroidal flux density at TF coil
B_c	peak poloidal flux density in the primary solenoid
β_I	poloidal (current) beta
$\langle\beta\rangle$	volume average beta
β^*	root mean square beta
β^*_{JET}	root mean square beta obtained in JET
c	capital cost per unit of engineered volume
e	plasma elongation
E_R	energy per reaction
E_α	α particle energy per reaction
f_I	α particle and impurity ion fraction
f_n	profile factor
F	power output fudge factor
I_p	plasma current
K	capital cost of engineered volume per unit thermal power
n	plasma fuel ion density
$\overline{n}$	volume averaged n
ν_n	density profile index
ν_T	temperature profile index
P_c	plasma chamber power flux (i.e. "wall loading")
P_T	reactor thermal power output
P_w	plasma surface power flux
P_n	chamber neutron wall loading
q_I	plasma edge safety factor (current averaged)
R	plasma major radius
$\langle\sigma\nu\rangle$	reaction rate parameter
t	engineered volume thickness
T	plasma ion temperature
T_n	density weighted volume averaged temperature
V	plasma volume
x	poloidal beta $\beta_I \alpha (R/a)^x$

HER MAJESTY'S STATIONERY OFFICE

Government Bookshops

49 High Holborn, London WC1V 6HB
(London post orders: PO Box 276, London SW8 5DT)
13a Castle Street, Edinburgh EH2 3AR
Brazennose Street, Manchester M60 8AS
Southey House, Wine Street, Bristol BS1 2BQ
258 Broad Street, Birmingham B1 2HE
80 Chichester Street, Belfast BT1 4JY

Publications may also be ordered through any bookseller